Physics Letters A 375 (2011) 614–619

Contents lists available at ScienceDirect

Physics Letters A

www.elsevier.com/locate/pla

First-principles study of monolayer and bilayer honeycomb structures of group-IV elements and their binary compounds

L. Pan [a], H.J. Liu [a,*], Y.W. Wen [a], X.J. Tan [a], H.Y. Lv [a], J. Shi [a], X.F. Tang [b]

[a] Key Laboratory of Artificial Micro- and Nano-structures of Ministry of Education and School of Physics and Technology, Wuhan University, Wuhan 430072, China
[b] State Key Laboratory of Advanced Technology for Materials Synthesis and Processing, Wuhan University of Technology, Wuhan 430072, China

ARTICLE INFO

Article history:
Received 30 August 2010
Received in revised form 19 November 2010
Accepted 29 November 2010
Available online 1 December 2010
Communicated by R. Wu

Keywords:
Honeycomb structures
Electronic properties
Phonon dispersion relations
Density functional calculations

ABSTRACT

By using first-principles pseudopotential method, we investigate the structural, vibrational, and electronic properties of monolayer and bilayer honeycomb structures of group-IV elements and their binary compounds. It is found that the honeycomb structures of Si, Ge, and SiGe are buckled for stabilization, while those of binary compounds SiC and GeC containing the first row elements C are planar similar to a graphene sheet. The phonon dispersion relations and electronic band structures are very sensitive to the number of layers, the stacking order, and whether the layers are planar or buckled.

1. Introduction

In recent years, graphene, a two-dimensional (2D) honeycomb structure of carbon, has attracted great interest in both theoretical and experimental study. With the significant advance in the fabrication and manipulation of graphene sheets, a lot of attention has been devoted to graphene with increasing number of layers [1–11]. Due to the unique structures and novel electronic properties, graphene and few-layer graphene (FLG) have been suggested as promising candidates for future nanoelectronics [2,6,12,13]. On the other hand, the vibrational properties of graphene are found to be sensitive to the number of layers and interlayer interactions [14–18].

While the investigation about graphene and graphene layers is growing rapidly, one has started to study the honeycomb lattices of other group-IV elements. Recently, Si and Ge monolayer honeycomb structures with a puckered geometry have been proposed [19–22] and are believed to be stable [23–25]. Besides, the formation of single- and double-layer nanofilms of Si have been predicated by molecular-dynamics (MD) simulations [26]. On the experimental side, single-crystal Si monolayer structures have been successfully realized through chemical exfoliation [27,28]. The honeycomb structures of group-IV binary compounds SiC and GeC have been also reported to exhibit interesting electronic properties [24,29–31]. To have a complete understanding of the honeycomb structures containing group-IV elements, in this work, we use density functional calculations to study the electronic and phonon properties of Si, Ge, SiGe, SiC, GeC with monolayer and bilayer structures. It should be mentioned that the focus of our work is on the bilayer systems, since some of the monolayer results have been previously found [24] and they are shown just for comparison and verification. Our results are also compared with those of graphene layers.

2. Computational details

Our total energy calculations have been performed by using a plane-wave pseudopotential formulation [32–34] within the framework of density functional theory (DFT). The code is implemented in the Vienna *ab initio* simulation package (VASP). The exchange-correlation energy is in the form of Ceperley–Alder [35] as parameterized by Perdew and Zunger [36]. The honeycomb structures are simulated by using a supercell geometry where the closest distance between the layer and its periodic image is set to 10 Å. The Brillouin zone is sampled with $20 \times 20 \times 1$ Monkhorst meshes. Optimal atomic positions are determined until the magnitude of the forces acting on all atoms becomes less than 0.05 eV/Å. On the other hand, the phonon calculations are performed by using the density functional perturbation theory (DFPT) which allows for accurate calculations of phonon modes at generic wave vectors. We use the so-called PWSCF code [37] where the Methfessel–Paxton smearing [38] with an energy width of 0.03 Ry and $16 \times 16 \times 1$ uni-

* Corresponding author.
E-mail address: phlhj@whu.edu.cn (H.J. Liu).

0375-9601/$ – see front matter
doi:10.1016/j.physleta.2010.11.062

form **k**-point mesh are adopted for the self-consistent calculations. To obtain the dynamical matrices, an $8 \times 8 \times 1$ grid of **q** points is used for the phonon calculations.

3. Results and discussions

We first discuss the structural properties of these honeycomb structures. Fig. 1(a) shows the relaxed geometry of monolayer SiGe compound, which forms a stable low-buckled (LB, or puckered) hexagonal structure [24]. The monolayer Si and Ge have similar structures and thus are not shown. In contrast, both the SiC and GeC monolayer exhibit planar (PL) hexagonal geometry [24]. As indicated in Fig. 1(b) and 1(c), there are two kinds of bilayer system. In the case of AB stacking, the atoms on top of each other are of different types, while they are the same for the AB′ stacking. We do not consider the AA stacking since such configuration in the graphite system is energetically unfavorable [39]. Of course, there is only AB′ stacking for the bilayer Si and Ge. It should be mentioned that for the bilayer SiGe compound, the atoms on top of each other in adjacent layers are covalently bonded which indicates a puckered sp^3 hybridization. This is however not the case for the bilayer SiC or GeC where the atoms remain the sp^2 hybridization, thus form a structure very similar to bilayer graphene. Table 1 summarizes the optimized lattice constant, buckling distance, interlayer spacing, and total energy for all the investigated structures. We see that the lattice constant and buckling distance of the monolayer systems are in good agreement with those found previously [23,24]. For the bilayer systems, the in-plane lattice constants are close to those of the corresponding monolayer structures, while there is an obvious increase of the buckling distances. For each system, the total energy is found to decrease from the monolayer to bilayer structure. Moreover, the AB stacking seems energetically more favorable than the AB′ stacking, especially for the bilayer SiGe compound.

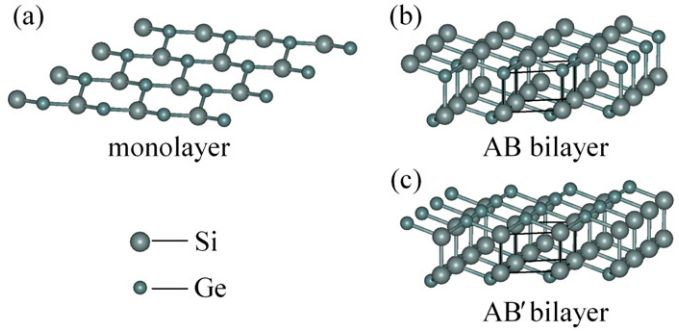

Fig. 1. Ball-and-stick model of (a) monolayer, (b) AB bilayer, and (c) AB′ bilayer for the SiGe honeycomb structures.

Fig. 2 shows the calculated phonon dispersion relations for both the monolayer and bilayer honeycomb structures of Si, SiGe, and SiC. We see that all of them (some being in LB and others in PL geometry) have positive phonon frequencies which indicate the stability of these honeycomb structures. We have also calculated the phonon dispersion relations for the Ge and GeC systems (not shown here), and the results are similar to those of the Si and SiC systems, respectively. In all the investigated systems, we see that the phonon dispersions for the in-plane LA and TA branches

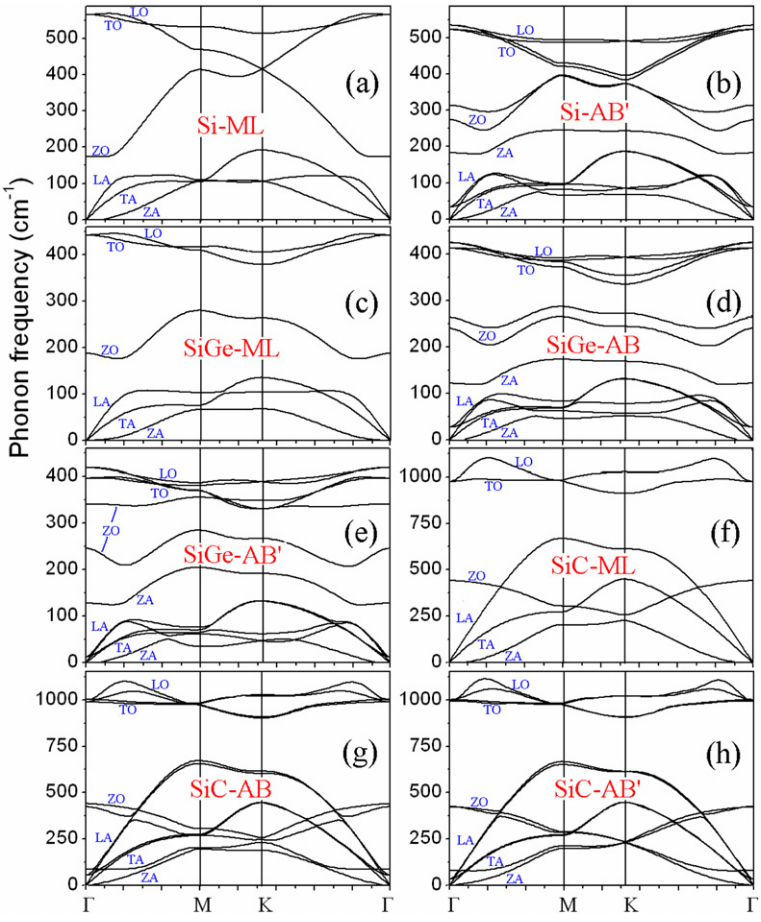

Fig. 2. (Color online.) Phonon dispersion relations for the honeycomb structures of: (a) monolayer Si, (b) AB′ bilayer Si, (c) monolayer SiGe, (d) AB bilayer SiGe, (e) AB′ bilayer SiGe, (f) monolayer SiC, (g) AB bilayer SiC, and (h) AB′ bilayer SiC.

Table 1
The optimized lattice constant a (Å), buckling distance Δ (Å), interlayer spacing d (Å), and the total energy E_0 (eV/atom) for the honeycomb structures of group-IV elements and their binary compounds.

	Si		Ge		SiGe			SiC			GeC		
	monolayer	AB′ bilayer	monolayer	AB′ bilayer	monolayer	AB bilayer	AB′ bilayer	monolayer	AB bilayer	AB′ bilayer	monolayer	AB bilayer	AB′ bilayer
a	3.86	3.84	4.04	3.97	3.94	3.92	3.90	3.05	3.05	3.05	3.19	3.19	3.19
Δ	0.44	0.64	0.68	0.74	0.57	0.68	0.75	–	–	–	–	–	–
d	–	3.12	–	3.35	–	3.23	3.20	–	3.18	3.40	–	3.50	3.36
E_0	−5.20	−5.39	−4.56	−4.73	−4.86	−5.03	−4.93	−7.71	−7.75	−7.74	−6.73	−6.76	−6.76

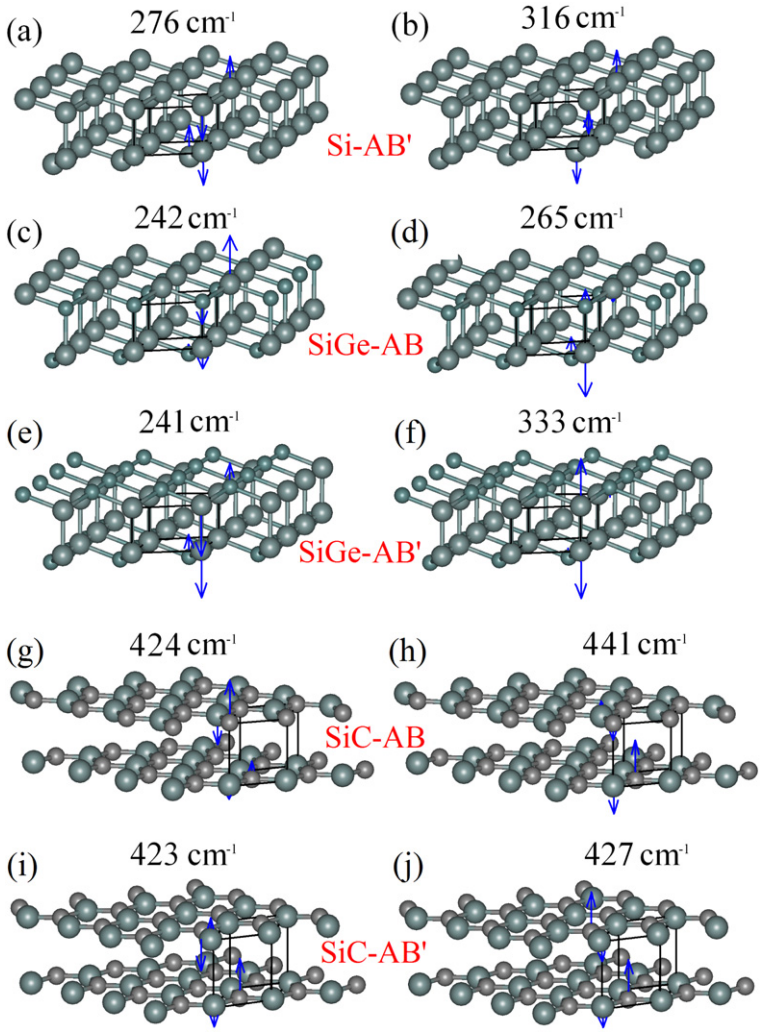

Fig. 3. (Color online.) Atomic displacements of the split ZO modes at the Γ point in the bilayer honeycomb structures: (a) and (b) for the AB′ bilayer Si, (c) and (d) for the AB bilayer SiGe, (e) and (f) for the AB′ bilayer SiGe, (g) and (h) for the AB bilayer SiC, (i) and (j) for the AB′ bilayer SiC. The length of the arrow represents the amplitude of the vibration.

are linear around the Γ point, while the out-of-plane ZA mode shows a quadratic dispersion. We first focus on the monolayer Si. We find that the calculated phonon spectrum shown in Fig. 2(a) agree well with previous result [24], which confirms the reliability of our calculations. The phonon dispersion exhibits some interesting features when we go from the monolayer to the bilayer Si. As shown in Fig. 2(b), there are obvious band-splittings of all the phonon branches, which is due to the symmetry breaking caused by interlayer coupling. In particular, the original ZO branch evolves into two branches with a large gap at the Γ point, and one additional ZA branch is found between the LA and ZO branches with frequency of about 183 cm^{-1} at the Γ point. The frequencies of LO and TO modes in the bilayer structure are obviously lower than those found in the monolayer, while the frequencies of ZO modes become higher. Such observation is distinct from that of graphene layers [15] and can be attributed to their distinct geometry differences.

Fig. 2(c) shows the calculated phonon dispersion for the monolayer SiGe, we see that the topology is similar to that of the monolayer Si (Fig. 2(a)). However, the ZO and TO branches do not cross at the K point due to relatively lower symmetry in SiGe structure. As shown in Fig. 2(d) and 2(e), the phonon branches also exhibit band-splitting in the bilayer SiGe compounds. The separation of ZO branches becomes even larger, and this is especially the case for the AB′ stacking where a frequency gap of about 70 cm^{-1} is found at the Γ point.

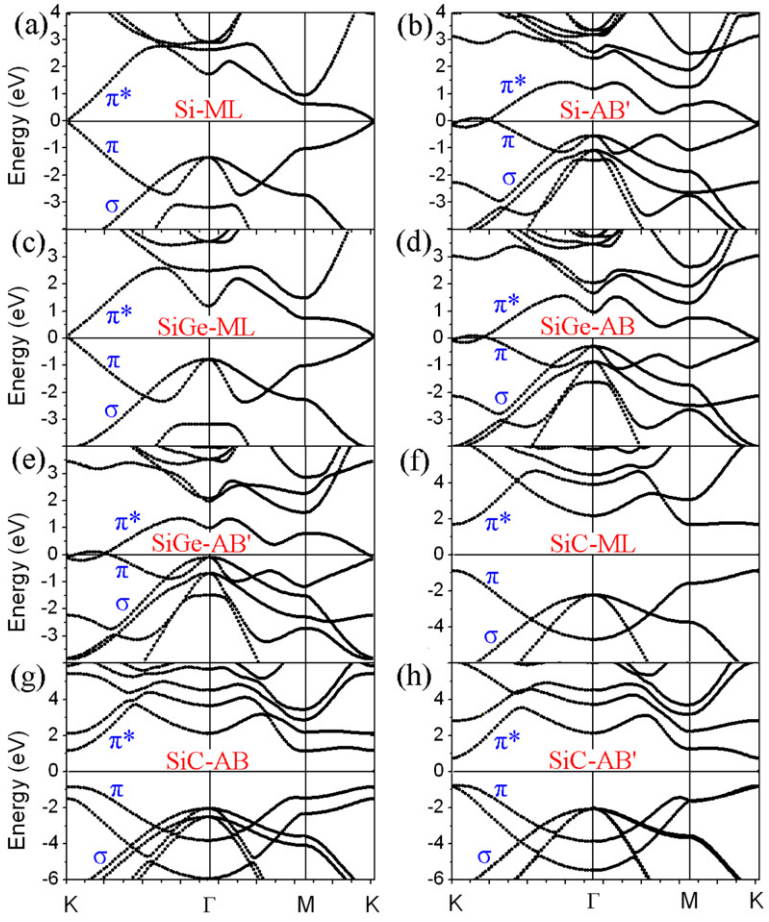

Fig. 4. (Color online.) Calculated band structures for the honeycomb structures of: (a) monolayer Si, (b) AB′ bilayer Si, (c) monolayer SiGe, (d) AB bilayer SiGe, (e) AB′ bilayer SiGe, (f) monolayer SiC, (g) AB bilayer SiC, and (h) AB′ bilayer SiC.

The phonon spectrum for the monolayer SiC is given in Fig. 2(f). We see that the overall topology is very similar to that found in a graphene sheet since the SiC layer is planar rather than buckled. Unlike the Si or SiGe system, the ZO branch of SiC layer falls in the frequency range of acoustical branches. The band-splittings in the bilayer SiC are however not that significant. As shown in Fig. 2(g) and 2(h), there is only a small split near the Γ point for the ZA branches. These features are also found in the graphene layers [15] but are not the cases for the Si or SiGe bilayers.

Fig. 3 schematically shows the atomic displacements of the ZO modes at the Γ point for all the bilayer systems mentioned above. The corresponding phonon frequencies are also indicated. In the case of bilayer Si, we see from Fig. 3(a) and 3(b) that the two bonded Si atoms within the same layer vibrate oppositely. On the other hand, the two Si atoms on top of each other in the adjacent layers vibrate either in the same direction (276 cm^{-1}) or the opposite direction (316 cm^{-1}), respectively. These findings indicate that the observed splitting of ZO branch in Fig. 2(b) is caused by strong interlayer interactions. The two split ZO modes at the Γ point for the bilayer SiGe are illustrated in Fig. 3(c) and 3(d) for the AB stacking, and Fig. 3(e) and 3(f) for the AB′ stacking. We see that the vibrations of two bonded atoms in the same layer or adjacent layer are similar to those of the bilayer Si. However, the amplitudes of the eigenvectors are different for the bonded Si and/or Ge atoms. Compared with that of the AB bilayer SiGe, it is clear that the larger split of ZO mode in the AB′ stacking (see Fig. 2(e)) is due to much stronger vibration of the two Si atoms on top of each other in the adjacent layers. As for the bilayer SiC, we see from Fig. 3(g)–3(j) that the interlayer vibrations are much weaker compared with those of bilayer Si and SiGe. In other words, the smaller band-splittings observed in the SiC bilayer (see Fig. 2(g) and 2(h)) is due to the weaker layer–layer interactions.

Table 2 summarizes the calculated Γ point frequency, mode symmetry, and optical activity of optical phonon for all the investigated monolayer and bilayer systems. The corresponding point group is also listed. We see that the point group is D_{3d} for both the monolayer and bilayer Si or Ge. Due to band-splitting, two more phonon modes are found in the bilayer Si or Ge with A_{2u} and E_u symmetries. Both of them are infrared (IR) active in contrast to the original A_{1g} and E_g modes with Raman active. For the binary compound SiGe, the point group is reduced to C_{3V}. Compared with the monolayer SiGe, the bilayer also has two more phonon modes (A_1 and E) which are both Raman and IR active. Moreover, the AB and AB′ stacking have obviously different phonon frequencies. For the SiC and GeC systems with planar geometry, we see from Table 2 that the point group is reduced from D_{3h} to C_{3V} for both the AB and AB′ stacking, where the four split phonon modes with A_1 or E symmetry are both Raman and IR active. In contrast, the mode symmetries in the monolayer counterpart are A_2'' (IR active) and E' (IR + Raman active). Our calculated results suggest that the number of layers and/or the stacking order can be experimentally obtained from the Raman and IR measurements.

We now move to the electronic properties. Fig. 4 plots the band structures of monolayer and bilayer Si, SiGe and SiC. We do not show the energy bands for the Ge and GeC since they are very similar to those of the Si and SiC, respectively. If we focus on the monolayer structures, it is interesting to note that the buckled Si and SiGe are half-metallic while the planar SiC is semiconducting

Table 2
The calculated Γ point frequency (in cm^{-1}), mode symmetry, and optical activity of optical phonon for the monolayer and bilayer Si, Ge, SiGe, SiC, and GeC. The corresponding point group is also listed.

	Si				Ge				SiGe				SiC				GeC			
	point group	frequency	symmetry	activity	point group	frequency	symmetry	activity	point group	frequency	symmetry	activity	point group	frequency	symmetry	activity	point group	frequency	symmetry	activity
monolayer	D_{3d}	174	A_{1g}	Raman	D_{3d}	160	A_{1g}	Raman	C_{3v}	188	A_1	IR + Raman	D_{3h}	442	A_2''	IR	D_{3h}	319	A_2''	IR
		576	E_g	Raman		310	E_g	Raman		443	E	IR + Raman		974	E'	IR + Raman		854	E'	IR + Raman
AB bilayer									C_{3v}	242	A_1	IR + Raman	C_{3v}	424	A_1	IR + Raman	C_{3v}	306	A_1	IR + Raman
										265	A_1	IR + Raman		441	A_1	IR + Raman		324	A_1	IR + Raman
										414	E	IR + Raman		987	E	IR + Raman		850	E	IR + Raman
										426	E	IR + Raman		1001	E	IR + Raman		863	E	IR + Raman
AB′ bilayer	D_{3d}	276	A_{2u}	IR	D_{3d}	179	A_{2u}	IR	C_{3v}	241	A_1	IR + Raman	C_{3v}	423	A_1	IR + Raman	C_{3v}	308	A_1	IR + Raman
		316	A_{1g}	Raman		193	A_{1g}	Raman		331	A_1	IR + Raman		427	A_1	IR + Raman		310	A_1	IR + Raman
		525	E_g	Raman		218	E_g	Raman		388	E	IR + Raman		991	E	IR + Raman		853	E	IR + Raman
		537	E_u	IR		295	E_u	IR		410	E	IR + Raman		1000	E	IR + Raman		862	E	IR + Raman

[24]. The band structures are very sensitive to the number of layers and their stacking order. For the monolayer Si and SiGe, the π and π^* bands crossing the Fermi level at the K point and have linear dispersions. For the bilayer Si and SiGe, these two bands cross the Fermi level not only at the K point, but also at about 1/4 KΓ from the K point. Due to strong interlayer interactions in the bilayer Si and SiGe, the original σ band is split into two bands and both the conduction and valence bands become closer to the Fermi level. For the AB′ stacking of SiGe bilayer, the valence band maximum at the Γ point is found to move to the Fermi level compared with that of the AB stacking. These findings are quite different from those in graphene layers [2] which have a planar geometry and very weak interlayer coupling.

As mentioned, the planar SiC systems are semiconducting with direct band gaps at the K point. The calculated gaps are 2.54 eV for the monolayer, which is higher than that of AB (1.98 eV) and AB′ bilayer (1.56 eV). It should be noted that LDA is known to underestimate the fundamental gap and one should be very careful when comparing with the experimental result. Usually a quasiparticle approach could give an improved predication of the band gap [40]. However, the basic physics reported here should not be changed. Unlike those found in Si or SiGe layers, we see from Fig. 4 that the π and π^* bands in the monolayer SiC no longer cross the Fermi level, and are split into two separate bands for the AB and AB′ bilayer. Similar features are also found in graphene layers [2] and again indicate the weak interaction between the SiC layers.

4. Summary

In summary, we have used density functional theory and density functional perturbation theory to study the monolayer and bilayer Si, Ge, SiGe, SiC and GeC in honeycomb structures. Compared with those found in graphene layers, these honeycomb structures exhibit distinct electronic and phonon properties with respect to the geometric configurations, the number of layers, and the stacking order, etc., and are believed to have potential applications in future nano-scale devices.

Acknowledgements

This work was supported by the “973 Program” of China (Grant No. 2007CB607501), the Program for New Century Excellent Talents in University, and the Natural Science Foundation for the Outstanding Young Scientists of Hubei Province. We also thank financial supports from the interdiscipline and postgraduate programs under the “Fundamental Research Funds for the Central Universities”. All the calculations were performed in the PC Cluster from Dawn Company of China.

References

[1] K.S. Novoselov, A.K. Geim, S.V. Morozov, D. Jiang, Y. Zhang, S.V. Dubonos, I.V. Grigorieva, A.A. Firsov, Science 306 (2004) 666.
[2] S. Latil, L. Henrard, Phys. Rev. Lett. 97 (2006) 036803.
[3] A.C. Ferrari, J.C. Meyer, V. Scardaci, C. Casiraghi, M. Lazzeri, F. Mauri, S. Piscanec, D. Jiang, K.S. Novoselov, S. Roth, A.K. Geim, Phys. Rev. Lett. 97 (2006) 187401.
[4] A. Gupta, G. Chen, P. Joshi, S. Tadigadapa, P.C. Eklund, Nano Lett. 6 (2006) 2267.
[5] C.L. Lu, C.P. Chang, Y.C. Huang, R.B. Chen, M.L. Lin, Phys. Rev. B 73 (2006) 144427.
[6] B. Partoens, F.M. Peeters, Phys. Rev. B 74 (2006) 075404.
[7] D. Graf, F. Molitor, K. Ensslin, C. Stampfer, A. Jungen, C. Hierold, L. Wirtz, Nano Lett. 7 (2007) 238.
[8] B. Partoens, F.M. Peeters, Phys. Rev. B 75 (2007) 193402.
[9] S. Latil, V. Meunier, L. Henrard, Phys. Rev. B 76 (2007) 201402(R).
[10] A. Das, S. Pisana, B. Chakraborty, S. Piscanec, S.K. Saha, U.V. Waghmare, K.S. Novoselov, H.R. Krishnamurthy, A.K. Geim, A.C. Ferrari, A.K. Sood, Nat. Nanotechnol. 3 (2008) 210.
[11] J. Hass, F. Varchon, J.E. Millán-Otoya, M. Sprinkle, N. Sharma, W.A. de Heer, C. Berger, P.N. First, L. Magaud, E.H. Conrad, Phys. Rev. Lett. 100 (2008) 125504.
[12] S.B. Trickey, F. Müller-Plathe, G.H.F. Diercksen, J.C. Boettger, Phys. Rev. B 45 (1992) 4460.
[13] J. Nilsson, A.H. Castro Neto, F. Guinea, N.M.R. Peres, Phys. Rev. B 78 (2008) 045405.
[14] J.W. Jiang, H. Tang, B.S. Wang, Z.B. Su, Phys. Rev. B 77 (2008) 235421.
[15] J.A. Yan, W.Y. Ruan, M.Y. Chou, Phys. Rev. B 77 (2008) 125401.
[16] S.K. Saha, U.V. Waghmare, H.R. Krishnamurthy, A.K. Sood, Phys. Rev. B 78 (2008) 165421.
[17] K.H. Michel, B. Verberck, Phys. Rev. B 78 (2008) 085424.
[18] J.A. Yan, W.Y. Ruan, M.Y. Chou, Phys. Rev. B 79 (2009) 115443.
[19] K. Takeda, K. Shiraishi, Phys. Rev. B 50 (1994) 14916.
[20] Y. Zhang, Y. W Tan, H.L. Stormer, P. Kim, Nature 438 (2005) 201.
[21] X.B. Yang, J. Ni, Phys. Rev. B 72 (2005) 195426.
[22] E. Durgun, S. Tongay, S. Ciraci, Phys. Rev. B 72 (2005) 075420.
[23] S. Cahangirov, M. Topsakal, E. Aktürk, H. Şahin, S. Ciraci, Phys. Rev. Lett. 102 (2009) 236804.
[24] H. Şahin, S. Cahangirov, M. Topsakal, E. Bekaroglu, E. Aktürk, R.T. Senger, S. Ciraci, Phys. Rev. B 80 (2009) 155453.
[25] M. Houssa, G. Pourtois, V.V. Afanas'ev, A. Stesmans, Appl. Phys. Lett. 96 (2010) 082111.
[26] T. Morishita, K. Nishio, M. Mikami, Phys. Rev. B 77 (2008) 081401(R).
[27] H. Nakano, T. Mitsuoka, M. Harada, K. Horibuchi, H. Nozaki, N. Takahashi, T. Nonaka, Y. Seno, H. Nakamura, Angew. Chem. 118 (2006) 6451.
[28] R. Krishnan, Q. Xie, J. Kulik, X.D. Wang, S. Lu, M. Molinari, Y. Gao, T.D. Krauss, P.M. Fauchet, J. Appl. Phys. 96 (2004) 654.
[29] L. Sun, Y. Li, Z. Li, Q. Li, Z. Zhou, Z. Chen, J. Yang, J.G. Hou, J. Chem. Phys. 129 (2008) 174114.
[30] E. Bekaroglu, M. Topsakal, S. Changirov, S. Ciraci, Phys. Rev. B 81 (2010) 075433.
[31] B. Xu, J. Yin, Y.D. Xia, X.G. Wan, Z.G. Liu, Appl. Phys. Lett. 96 (2010) 143111.
[32] G. Kresse, J. Hafner, Phys. Rev. B 47 (1993) 558.
[33] G. Kresse, J. Hafner, Phys. Rev. B 49 (1994) 14251.
[34] G. Kresse, J. Furthmüller, Comput. Mater. Sci. 6 (1996) 15.
[35] D.M. Ceperley, B.J. Alder, Phys. Rev. Lett. 45 (1980) 566.
[36] J.P. Perdew, A. Zunger, Phys. Rev. B 23 (1981) 5048.
[37] S. Baroni, A. Dal Corso, S. De Gironcoli, P. Giannozzi, http://www.pwscf.org.
[38] M. Methfessel, A.T. Paxton, Phys. Rev. B 40 (1989) 3616.
[39] J.C. Charlier, J.P. Michenaud, X. Gonze, Phys. Rev. B 46 (1992) 4531.
[40] B. Baumeier, P. Krüger, J. Pollmann, Phys. Rev. B 76 (2007) 085407.